Nitric oxide is essential for cadmium-induced peroxule formation and peroxisome proliferation

Laura C. Terrón-Camero[1], María Rodríguez-Serrano[1,2], Luisa M. Sandalio[1], María C. Romero-Puertas[1*].

[1] Departamento de Bioquímica, Biología Celular y Molecular de Plantas, Estación Experimental del Zaidín, CSIC, Profesor Albareda 1, E-18008 Granada, Spain;

[2] Present address:

*Author for correspondence:

Dr. María C. Romero-Puertas,

Departamento de Bioquímica, Biología Celular y Molecular de Plantas,

Estación Experimental del Zaidín, CSIC, Apartado 419, E-18080 Granada, SPAIN.

Tel: +34 958 181600 Ext.175, 299

maria.romero@eez.csic.es

Running title: NO function in peroxisome dynamic and metabolism

Research area: Environmental stress and adaptation

Keywords: cadmium; carbonylation; catalase; nitric oxide; peroxisomes; peroxules; signalling; *S*-nitrosylation

ABSTRACT

Nitric oxide (NO) and nitrosylated derivatives are produced in peroxisomes, but the impact of NO metabolism on organelle functions remains largely uncharacterised. Double and triple NO-related mutants expressing cyan florescent protein (CFP)-SKL (*nox1* x *px-ck* and *nia1 nia2* x *px-ck*) were generated to determine whether NO regulates peroxisomal dynamics in response to cadmium (Cd) stress using confocal microscopy. Peroxule production was compromised in the *nia1 nia2* mutants, which had lower NO levels than the wild type plants. These findings show that NO is produced early in the response to Cd stress and was involved in peroxule production. Cd-induced peroxisomal proliferation was analysed using electron microscopy and by the accumulation of the peroxisomal marker PEX14. Peroxisomal proliferation was inhibited in the *nia1 nia2* mutants. However, the phenotype was recovered by exogenous NO treatment. The number of peroxisomes and oxidative metabolism were changed in the NO-related mutant cells. Furthermore, the pattern of oxidative modification and *S*-nitrosylation of the catalase (CAT) protein was changed in the NO-related mutants in both the absence and presence of Cd stress. Peroxisome-dependent signalling was also affected in the NO-related mutants. Taken together, these results show that NO metabolism plays an important role in peroxisome functions and signalling.

INTRODUCTION

Peroxisomes are single membrane-bound organelles that generate reactive oxygen species as by-products of normal cellular metabolism (Hu *et al.* 2012). The morphology, number and metabolism of these dynamic organelles adapt to the tissue, organs and nutritional state of the plant. In plants, peroxisomes play a crucial role in different biochemical pathways, including photorespiration, fatty acid β-oxidation, glyoxylate metabolism, amino-acid catabolism, polyamine oxidation and hormone biosynthesis (Reumann & Bartel 2016). While their metabolic processes are remarkable in their variety and plasticity, using omics techniques, recent studies have uncovered new functions in these plant peroxisomes (Reumann & Bartel 2016). Peroxisomes are also a key source of reactive oxygen and nitrogen species (ROS/RNS), whose accumulation is regulated by a wide range of antioxidant defences (Sandalio & Romero-Puertas 2015). Overproduction of ROS and RNS, which act as signals to regulate developmental processes and stress responses at low level, can cause severe cellular oxidative and nitrosative stress (Marinho, Real, Cyrne, Soares & Antunes 2014; Mittler 2017; Castillo, Coego, Costa-Broseta & León 2018). In addition, peroxisomes play an important role in cellular redox homeostasis, which, in turn, is crucial for the regulation of cellular metabolic pathways (Foyer & Noctor 2003; Yun, Spoel & Loake 2012). ROS also regulate rapid changes in peroxisomal metabolism and dynamics caused by the environment (Rodríguez-Serrano *et al.* 2009; Sinclair, Trobacher, Mathur, Greenwood & Mathur 2009; Hu *et al.* 2012; Kao, Gonzalez & Bartel 2018), suggesting that these organelles may be involved in important cellular decision-making platforms (Sandalio & Romero-Puertas 2015).

We previously showed that the toxic heavy metal cadmium (Cd), which causes major environmental and health concerns worldwide, produces time course-dependent

changes in peroxisomal dynamics. Specifically, peroxisomal membrane extensions (peroxules) were initially observed, followed by peroxisome proliferation, with peroxisome numbers finally returning to those recorded under control conditions together with an increase in their speed of movement (Rodríguez-Serrano, Romero-Puertas, Sanz-Fernández, Hu & Sandalio 2016). While these changes are mainly regulated by NADPH oxidase (C and F)-related ROS production, peroxin 11a (PEX11a) was found to be essential for peroxule production (Rodríguez-Serrano *et al.* 2016). The results for PEX11a mutants suggested that peroxules are involved in regulating ROS accumulation and ROS-dependent gene expression in response to stress. These findings demonstrate that PEX11a and peroxule formation play a key role in regulating stress perception and rapid cell responses to environmental cues (Rodríguez-Serrano *et al.* 2016; Fransen, Lismont & Walton 2017).

The free radical nitric oxide (NO) acts as a ubiquitous inter- and intra-cellular signalling molecule involved in the regulation of plant stress responses and plant development (Yu, Lamattina, Spoel & Loake 2014; Sanz *et al.* 2015; León, Costa & Castillo 2016). NO has the capacity to regulate processes, such as hormonal metabolism and signalling, directly through protein post-translational modifications (PTMs), including *S*-nitrosylation (nitrosation) and nitration, which affect protein function, stability and localization (Martínez-Ruiz, Cadenas & Lamas 2011; Kovacs & Lindermayr 2013; Romero-Puertas & Sandalio 2016). In addition, NO reacts rapidly with reactive oxygen species (ROS) and also regulates ROS production and removal through the protein post-translational modification of enzymatic sources and antioxidant systems, respectively (Lindermayr & Durner 2015; Romero-Puertas & Sandalio 2016). NO also regulates peroxisomal proteins, antioxidants and ROS-producing compounds under both normal and stressful conditions caused by heavy

metals such as Cd (Gupta & Sandalio 2012; Ortega-Galisteo *et al.* 2012; Sandalio, Gotor, Romero & Romero-Puertas 2019).

Although NO has recently been found to be involved in plant responses to Cd and to provide overall stress protection, the mechanisms underlying its endogenous production in plants remain unclear (Romero-Puertas, Terrón-Camero, Peláez-Vico, Olmedilla & Sandalio 2019). The overall tendency for endogenous NO production to increase in plant responses following short-term treatments changes following long-term treatment (Terrón-Camero, Peláez-Vico, Del Val, Sandalio & Romero-Puertas 2019). It has been suggested that NO is linked to certain functions in plant responses to Cd, with transcriptomic analysis indicating that modulations in NO levels during plant responses to Cd stress are specifically involved in regulating root growth, nitrogen assimilation, iron homeostasis and metabolic proteolysis (Besson-Bard *et al.* 2009; Romero-Puertas *et al.* 2019). However, little is known about the role of nitric oxide in peroxisomal metabolism and dynamics during plant responses to Cd stress.

Using genetic and biochemical techniques, as well as NO donors and scavengers, we analysed peroxisomal metabolism and dynamics in plant responses to Cd stress. Two previously characterized mutants were used in this study: a mutant, whose NO production is impaired in nitrate reductases (NR1/NIA1and NR2/NIA2; *nia1 nia2*), which have been reported to play a role in NO biosynthesis (Yamasaki & Sakihama 2000; Rockel, Strube, Rockel, Wildt & Kaiser 2002; Desikan, Griffiths, Hancock & Neill 2002; Guo, Okamoto & Crawford 2003; Modolo, Augusto, Almeida, Magalhaes & Salgado 2005; Moreau, Lee, Wang, Crane & Klessig 2008); and a NO-overproducing mutant impaired in a chloroplast phosphoenolpyruvate/phosphate translocator (*nox1/cue1*; Streatfield *et al.* 1999; He *et al.* 2004). Our results suggest that NO regulates peroxule production and peroxisome proliferation in cell responses to Cd

stress. Peroxisome numbers and peroxisomal ROS-related metabolism were also affected by changes in NO levels in the plant.

MATERIALS AND METHODS

Plant material and growth conditions

Arabidopsis thaliana (Col-0) was the genetic background used in this study. Arabidopsis seeds (WT, *px-ck*, *nia1 nia2*, *nia1 nia2* x *px-ck*, *nox1* and *nox1* x *px-ck*) were surface sterilized and stratified for 48 hours at 4ºC and then sown on Hoagland solid medium (0.5x) with a pH of 5.6 (Hoagland & Arnon 1950). The seeds were grown at 22ºC, an irradiance of 100 µE and 60-65% relative humidity under 16/8 h light/dark conditions for 14 d. The seedlings were then transferred to Petri dishes with 9 ml of liquid Hoagland (0.5x) medium, and the roots of 15 seedlings were submerged for 24 h under hydroponic conditions. Subsequently, the initial Hoagland (0,5x) medium was replaced by 9 ml of liquid Hoagland medium containing 100 µM $CdCl_2$ and the seedlings were harvested at 30 min, 1 h and 3 h, weighed and processed or frozen when necessary. *S*-nitrosoglutathione (GSNO; 1 mM and 0,25 mM) as NO donor and 2-(4-Carboxyphenyl)-4,4,5,5-tetramethylimidazoline-1-oxyl-3-oxide (cPTIO) potassium salt (0.5 mM) as NO scavenger were freshly prepared and added to the medium when indicated.

Generation of double and triple mutants with altered NO levels and peroxisome-targeted CFP

Emasculated flowers from *nia1 nia2* (Wilkinson & Crawford 1993) and *nox1* (He *et al.* 2004) were crossed with pollen from *px-ck* containing a peroxisome-targeted cyan fluorescent protein (CFP) (Nelson, Cai & Nebenführ 2007). Emasculated flowers from *px-ck,* which were also crossed with pollen from *nia1 nia2* or *nox1,* produced similar results. F1 plants were self-pollinated, and double (*nox1* x *px-ck*) and triple

mutants (*nia1 nia2* x *px-ck*) were selected from F2 and F3 plants using fluorescence microscopy and then genotyped by PCR. The primers for *nia1 nia2* selection are described by Lozano-Juste & Leon 2010, the *CUE1* gene was deleted in *nox1* mutant and homozygous plants were selected as described elsewhere (He *et al.* 2004).

Confocal Microscopy Analyses

The leaves, all the same age, in the experiments belonged to plants grown under similar conditions. Arabidopsis leaves were sliced and mounted in 30:70% (v/v) PBS/glycerol as described elsewhere (Rodríguez-Serrano *et al.* 2016). The abaxial sections were examined using a TCS SP5 confocal laser scanning microscope (Leica Microsystems, Wetzlar, Germany). A minimum of seven confocal images were taken of one leaf of each plant, with at least five plants being used per experiment. Five independent experiments were carried out. At least 125 images per treatment were analyzed, meaning that thousands of peroxisomes were examined. The videos were generated by sequential images, with 15 frames being taken in the x, y, and t dimensions, and the number of peroxisomes and peroxules was analyzed using Leica Lite software (Leica Microsystems; Rodríguez-Serrano *et al.* 2016).

Gene Expression by qRT-PCR

Total RNA was isolated using Trizol reagent (Invitrogen), and DNase was used according to the manufacturer's protocol (Ambion DNA-free). 1 µg RNA was reverse transcribed with 5x PrimeScript RT Master Mix (Takara) as described elsewhere (Rodríguez-Serrano *et al.* 2016). Quantitative real-time PCR was performed on an iCycler iQ5 (Bio-Rad, Hercules, CA) using TB Green Premix Ex Taq (Takara). Amplification efficiency was calculated using the formula $E = [10\ (1/a)\ -1] \times 100$, where a is the slope of the standard curve. The relative expression of each gene was normalized to that of *TUB4*, and the results were analyzed using the method described

by Pfaffl (2001). The *TUB4* gene was selected for normalization by the GrayNorm algorithm (Remans *et al.* 2014) from five candidate reference genes as described previously (Terrón-Camero, Del Val, Sandalio & Romero-Puertas 2019). The stability of *TUB4* was checked under our conditions in all backgrounds (Suppl. Fig. S1). The primers used in this study are described in Suppl. Tables S1 and S2.

Enzymatic and Western blot analyses

Whole seedlings were homogenized as described elsewhere (Rodríguez-Serrano *et al.* 2016). Proteins were quantified using Bradford Protein Assay (Bio-Rad) and bovine serum albumin (BSA) was used in the standard curve. Extracts were used to measure catalase (CAT; EC 1.11.1.6) activity as described elsewhere (Aebi 1984). For the detection of carbonylated catalase, immunoprecipitation of derivatized proteins with dinitrophenyl hydrazine (DNPH) using an anti-DNPH antibody (1:40000 dilution) and subsequent immune detection with an anti-catalase antibody (1:5000; Agrisera) were performed (Romero-Puertas, Palma, Gómez, Del Río & Sandalio 2002). The biotin switch method was used to detect *S*-nitrosylated catalase (Romero-Puertas *et al.* 2007). The anti-biotin antibody (1:10,000; Sigma-Aldrich) was used to immunoprecipitate *S*-nitrosylated proteins followed by identification of CAT with an anti-catalase antibody (1:5000; Agrisera). An anti-PEX14 antibody (1:10.000; Agrisera) was used as a marker of peroxisomal accumulation (Calero-Muñoz *et al.* 2019).

H_2O_2 and NO detection

To detect nitric oxide, the seedling roots were incubated with 10 μM 4,5-diaminofluorescein diacetate (DAF-2 DA) as described previously (Terrón-Camero, Molina-Moya, Sanz-Fernández, Sandalio & Romero-Puertas 2018). The specificity of the reaction was checked by pre-incubating samples with the NO scavenger cPTIO (500 μM). Aminoguanidine (AG; 0.5 mM) and tungstate (TUNG; 0.5 mM) were used as

inhibitors of NOS-like and nitrate reductase activities, respectively, to identify the possible NO source. GSNO (1 mM) was used as a NO donor when described. Hydrogen peroxide (H_2O_2) was measured by fluorimetry using homovanillic acid (excitation: 315 nm; emission: 425 nm) and horseradish peroxidase in 50 mM HEPES pH 7.5 (Romero-Puertas *et al.* 2004). A standard curve of commercial H_2O_2 was used to quantify the samples. For NO detection, the seedling extracts were incubated with 20 μM DAF-2 for 2h at 37ºC (excitation: 495; emission: 515; Nakatsubo *et al.* 1998).

Cytochemical identification of peroxisomes

Cytochemical localization of peroxisomes was carried out as described elsewhere (Calero-Muñoz *et al.* 2019). All the leaves from the different genotypes were 15 days old and *nox1* x *px-ck* leaves were slightly smaller than *px-ck* leaves at this stage. Briefly, Arabidopsis leaves from *px-ck; nia1 nia2* x *px-ck* and *nox1* x *px-ck* seedlings were cut into pieces of approximately 1 mm^2 and initially fixed with 0.5% glutaraldehyde (v/v), prepared in 50 mM potassium phosphate buffer, pH 6.8, for 2.5 hours at RT. The pieces were then washed with the same buffer. The samples were incubated in DAB solution (2 mg/ml) prepared in 50 mM Tris-HCl, pH 9.0 for 1.5 hours. The samples were then incubated in a freshly prepared solution of DAB and 0.02% H_2O_2 at 37 °C for 3 h. Samples were subsequently washed with 50% potassium phosphate buffer, pH 6.8, and stained with 1% (w/v) OsO_4. The samples were then dehydrated in a stepped ethanol series from 30 to 100%. Once the samples were embedded in Spurr resin, semithin and ultrathin sections were obtained and contrasted for the analysis of the structure and ultrastructure by a light or transmission electron microscope (Zeiss ME 10C). The images were analyzed using Image-J (Fiji) software.

Statistical Analyses

Mean values for the quantitative experiments described above were obtained from at least three independent experiments with no less than three independent samples per experiment. Statistical analyses were performed using a one- or two-way ANOVA test when necessary followed by a Student´s t-test (p-value < 0.05) or Tukey multiple comparison test (p-value < 0.05), respectively. Analyses were carried out using IBM SPPS Statistic 24 and GraphPad Prism 6. Error bars representing standard error (SEM), as well as whiskers (maximum and minimum), are shown in the figures.

RESULTS

Peroxule production in response to Cd in NO-related mutants

Cd has recently been shown to induce peroxisomal membrane extensions, (peroxules) very soon after treatment, followed by peroxisome elongation, with constriction, beading and fragmentation into new peroxisomes giving rise to peroxisome proliferation at 3 h (Rodríguez-Serrano *et al.* 2016). To assess the possible involvement of nitric oxide (NO) in the morphological changes observed in peroxisomes in response to Cd, we first analysed the production of NO at the time these changes occurred (0-3 h). We observed a roughly 1.8-fold increase in NO in WT seedlings after 30 min. and a 1.5-increase after 3h of treatment with respect to control samples (Fig. 1). We also observed a significant increase in NO production in response to Cd stress in NO-related mutants *nia1 nia2*, which affected nitrate reductases (NR1/NIA1 and NR2/NIA2) and the NO overproducer, *nox1/cue1* (henceforth *nox1*; Fig. 1), although *nia1 nia2* showed lower and *nox1* higher NO levels as compared to WT plants (Fig. 1). These results suggest that nitrate reductase (NR) may not be the only source involved in increasing NO in the response of seedlings to Cd, although NO levels were highly compromised in *nia1 nia2* mutants. Furthermore, we used the NOS-l inhibitor aminoguanidine to

243 decrease NO production in seedling roots in response to Cd and the NR inhibitor
244 tungstate to increase NO production in response to Cd (Suppl. Fig. S2).

245 To monitor peroxisomal dynamics, we crossed *nia1 nia2* and *nox1* with the
246 peroxisomal marker line *px-ck*, giving rise to the triple *nia1 nia2 x px-ck* and double
247 *nox1 x px-ck* mutants, respectively. The *px-ck* line showed a slight increase in
248 fluorescence respect to WT, which may be due to the CFP protein (Suppl. Fig. S3A).
249 All the *px-ck* lines showed an increase in NO production in response to Cd (30 min),
250 similar to that observed in the non-*px-ck* lines (Suppl. Fig. S3B) and the trend in NO in
251 plant responses to Cd remained unchanged. We then observed peroxule production in
252 all *px-ck* lines at 30 min (Fig. 2A), when Arabidopsis showed a higher percentage of
253 peroxule-producing peroxisomes following Cd stress (Rodríguez-Serrano et al., 2016),
254 which matches the increase in NO production observed in Fig. 1. To determine whether
255 NO is involved in peroxule formation, we treated Arabidopsis plants with the NO
256 scavenger carboxy-2-phenyl-4,4,5,5-tetramethy-limidaziline-1-oxyl-3-oxide (cPTIO),
257 which has previously been shown to decrease NO accumulation in response to Cd
258 (Besson-Bard et al. 2009). The cPTIO scavenger caused a decrease of 75% in the
259 number of peroxule-extending peroxisomes in response to Cd (Fig. 2B). Interestingly,
260 peroxule formation decreased sharply by approximately 75% in response to Cd in *nia1*
261 *nia2 x px-ck* as compared to *px-ck* mutants (Fig. 2A and C; Suppl. Videos S4 and S5),
262 with peroxule-producing peroxisomes (in green) accounting for only 5% of the total
263 (Fig. 2A, 2C and Suppl. Video S5). No significant level of peroxule production was
264 found in any of the backgrounds analysed under control conditions (Suppl. Videos S1-
265 S3). Furthermore, the percentage of peroxule-producing peroxisomes increased to 18%
266 when *nia1 nia2 x px-ck* plants were simultaneously incubated with Cd and the NO
267 donor GSNO (Fig. 2C; Suppl. Video S6), similar to the percentage of peroxules in *px-ck*

under Cd stress (Fig. 2C). Other NO donors, such as N-Acetyl-3-(nitrosothio)-DL-valine and S-Nitroso-N-acetylpenicillamine (SNAP), were also able to induce peroxule production (data non shown). No increase in peroxule production was observed in WT incubated with GSNO and Cd simultaneously (Fig. 2C; Suppl. Video S5), suggesting that a minimum amount of NO is needed to reach the percentage of peroxule production required in response to Cd and that an excess of NO does not increase peroxule production. In fact, the level of peroxule production in *nox1* x *px-ck* mutants, with their increased levels of NO, did not differ significantly from that observed in *px-ck* mutants (Fig. 2A, 2C and Suppl. Video S8). We then checked peroxin 11a (*PEX11a*) expression, which has been shown to regulate peroxule production (Rodríguez-Serrano *et al.* 2016). Cd treatment was found to induce PEX*11a* in WT seedlings, which also occurred in *px-ck* mutants, suggesting that CFP does not alter PEX11a-dependent signalling (Suppl. Fig. S4). However, no significant changes in the *PEX11a* transcript were observed *in nia1 nia2* or *nox1* seedlings (Fig. 3), indicating that gene induction is not essential for peroxule production.

Peroxisome proliferation in plant responses to Cd in NO-related mutants

To assess whether peroxisome proliferation in response to Cd is also affected by NO, we used DAB histochemistry (Castillo, Sandalio, del Río & León 2008) and light microscopy to image and count the peroxisomes in cross sections of *nia1 nia2* x *px-ck*, *nox1* x *px-ck* and *px-ck* leaves (Suppl. Fig. S5). An increase in the number of peroxisomes per cell slice was observed in response to Cd in *px-ck* and *nox1* x *px-ck* mutants but not in *nia1 nia2 x px-ck* mutants (Fig. 4A). We then treated *nia1 nia2* mutants simultaneously with the NO donor GSNO and Cd and analysed the protein accumulation of peroxin 14 (PEX14), used as a marker of peroxisome accumulation, which was observed to increase after 3 h of Cd treatment (Calero-Muñoz *et al.* 2019).

PEX14 protein accumulation increased in *nia1 nia2* mutants after treatment with Cd and GSNO (3 h; Fig. 4B, Suppl. Fig. S6), which restored the WT phenotype.

Interestingly, the number of peroxisomes per cell slice under normal conditions was lower in *nox1* x *px-ck* mutants than in *px-ck* mutants (Fig. 4A). The distribution of peroxisomes per cell slice was also altered in *nox1* x *px-ck* mutants, with a 1.7-fold increase observed in the number of cells containing one peroxisome as compared to *px-ck* mutants*;* the number of cells containing three peroxisomes was 0.5-fold higher in *nox1* x *px-ck* mutants (Fig. 4C), and few cells contained more than three peroxisomes (Fig. 4C). The number of peroxisomes per cell was altered in *nia1 nia2 x px-ck* mutants, with an increase observed in cells containing one peroxisome, while those containing two peroxisomes decreased with respect to *px-ck* mutants (Fig. 4C).

Peroxisome morphology in mutants with altered NO-metabolism

Given that the number of peroxisomes per cell was different in mutants with altered NO-metabolism, we used electron microscopy to examine peroxisome morphology (Fig. 5A-F). Although *nox1* x *px-ck* leaves are slightly smaller than px-*ck* leaves, we observed no significant differences in peroxisome size in any of the NO-dependent mutants as compared to *px-ck* mutants (Fig. 5A, B, C and G). The area of peroxisomes in *px-ck* mutants is approximately 0.4-0.5 μm^2, which is similar to WT plants, showing that the presence of CFP does not affect the size of peroxisomes (Castillo et al., 2008). Circularity is lower under control conditions, in *nia1 nia2 x px-ck* than in *px-ck*, and slightly, but not significantly, higher in *nox1* x *px-ck* lines (Fig. 5A, B, C and H). We also observed a 7-fold increase in the number of *px-ck* peroxisomes with precipitates following Cd treatment (Fig. 5A, D and I), which, as reported elsewhere, is associated with CAT (Shibata *et al.* 2013) and/or H_2O_2 oxidization (Romero-Puertas *et al.* 2004). Interestingly, 25% of peroxisomes in *nia1 nia2 x px-ck*

mutants and 60% of those in *nox1* x *px-ck* mutants contained these precipitates under control conditions (Fig. 5A, B, C and I), suggesting that oxidative metabolism may be affected in both mutants. An increase in the number of peroxisomes containing precipitates was observed in both these mutants following Cd treatment, being similar to *px-ck* under the same conditions in *nia1 nia2 x px-ck* and double in *nox1* x *px-ck* (Fig. 5D, E and I).

Oxidative metabolism in NO-related mutants under Cd stress

Although H_2O_2 content did not change significantly in WT seedlings, it was found to decrease sharply in *nox1* after 1 h of treatment, while control levels recovered after 3 h (Fig. 6A). Similarly, in *nia1 nia2* mutants, a slight, but significant, decrease was observed after 1 h of Cd treatment, which was sustained for up to 3 h (Fig. 6A). In addition, *GST* expression, a gene marker of H_2O_2-dependent signalling, was induced in WT seedlings following Cd treatment (3 h) but not in *nox1* mutants (Fig. 6B). *GST* was induced in *nia1 nia2* mutants from the very beginning of treatment, with a significant down-regulation of *GST* expression observed in these mutants as compared to WT seedlings under control conditions (Fig. 6B). We then examined the peroxisomal enzyme catalase (CAT), which maintains H_2O_2 homeostasis. While a decrease in CAT activity was observed in WT in response to Cd stress (Fig. 6C), *CAT2* gene expression remained unchanged (Fig. 6D). CAT activity was also observed to decrease in the *nox1* mutants following Cd treatment but recovered significantly after 30 minutes (Fig. 6C), which was probably due to the initial induction of *CAT2* gene (Fig. 6D). Under control conditions however, CAT activity in *nox1* mutants was half that in WT seedlings. Interestingly, in *nia1 nia2* mutants, CAT activity and *CAT2* expression were double the levels observed in WT under control conditions (Fig. 6C-D). Though found to decrease in *nia1 nia2* mutants after Cd treatment, CAT activity was similar to that observed in

343 WT seedlings under control conditions (Fig. 6C). In addition, *CAT2* expression in *px-ck*
344 lines was not found to differ from that in WT plants in the plant response to Cd,
345 suggesting that the differences observed in NO-related mutants are due to their genotype
346 and not to the presence of CFP (Suppl. Fig. S4). Similar results were observed for
347 glycolate oxidase, one of the principal peroxisomal enzymes involved in H_2O_2
348 production (Suppl. Fig. S4).

349 **Post-translational modifications of catalase in mutants with altered NO**
350 **metabolism**

351 A decrease in CAT activity was observed, especially after 30 minutes of Cd
352 treatment, which does not appear to be due to any differences in *CAT2* expression in
353 WT plants. As CAT has been shown to be highly regulated by post-translational
354 modifications (PTMs), we analysed the oxidized and *S*-nitrosylated patterns of this
355 protein under control and Cd treatment conditions. We observed an increase in the
356 carbonylation of catalase, which is used as a marker of protein oxidation status, while
357 the pattern of *S*-nitrosylation did not change significantly under Cd treatment conditions
358 in WT seedlings as compared to non-treated seedlings (Fig. 7A and B). Interestingly,
359 given the highly oxidized and *S*-nitrosylated activity of CAT in *nia1 nia2* under control
360 conditions, a decrease in both these PTMs was observed in response to Cd treatment
361 (Fig. 7A and B). In *nox1* mutants however, the basal levels of *S*-nitrosylation, which
362 were maintained after Cd treatment, were higher than those observed in WT seedlings
363 (Fig. 7B), while, contrary to the behaviour of WT, oxidation status decreased (Fig. 7A).
364 CAT content remained unchanged after 30 minutes of Cd treatment in all Arabidopsis
365 backgrounds, although CAT content in *nia1 nia2* mutants was higher than that in WT
366 and *nox1* mutants (Suppl. Fig. S7).

367 **Peroxisome-dependent signalling in response to Cd**

As altered peroxisomal dynamics in mutants disrupt peroxisomal ROS-dependent signalling (Rodríguez-Serrano *et al.* 2016), we needed to determine whether peroxisome-dependent signalling is modified in NO-related mutants. We examined two genes, which are specifically up-regulated following peroxisomal H_2O_2 production (Sewelam *et al.* 2014) and associated with protein folding and repair: the heat shock protein 20-like (*HSP20-like*) gene and the Arabidopsis orthologs gene of the human Hsp70-binding protein (*FES1A*). The very early responses of these genes were found to be affected in both mutants as opposed to WT, which could be due to altered peroxisomal ROS metabolism rather than peroxule production (Fig. 8). Interestingly, although gene induction in *nia1 nia2* mutants after 3 hours of treatment was similar to that in WT, it was significantly lower in *nox1* mutants (Fig. 8).

DISCUSSION

Peroxisomes, which are essential organelles widely found in organisms ranging from yeast to mammals and particularly in plants, are involved in responses to different stresses (Baker & Paudyal 2014; Fransen *et al.* 2017; Mathur, Shaikh & Mathur 2018). Although the signalling molecule NO is involved in plant responses to Cd (Besson-Bard *et al.* 2009; Rodríguez-Serrano *et al.* 2009) and while peroxisomes are intimately related to NO metabolism (Sandalio & Romero-Puertas 2015), little is known about NO function in peroxisomal metabolism and dynamics under control and stress conditions.

NO regulates peroxule production in plant responses to Cd stress

We observed an increase in NO production in early responses (30 min to 3 h) to Cd in Arabidopsis seedlings (Fig. 1). This finding is in line with most studies of the response of NO production to short-term Cd treatment in a wide-range of plant species, although NO tends to decrease after long-term Cd treatments (Bartha, Kolbert & Erdei 2005; Groppa, Zawoznik, Tomaro & Benavides 2008; Besson-Bard *et al.* 2009;

Romero-Puertas *et al.* 2019; Terrón-Camero et al. 2020). We also observed an increase in NO in response to Cd in *nia1 nia2* mutants, whose NO production however is highly compromised with respect to WT seedlings (Fig. 1), with NR observed to be partly involved in the induction of NO in WT. Other sources may also be involved in NO induction following Cd treatment, after which incubation with the arginine competitor, aminoguanidine (AG), was found to diminish NO production (Suppl. Fig. S2). Results obtained with different species point to crosstalk between different NO sources in plant responses to Cd (Besson-Bard *et al.* 2009; Rodríguez-Serrano *et al.* 2009; Pérez-Chaca *et al.* 2014; Chen *et al.* 2018; Terrón-Camero et al. 2020; Terrón-Camero *et al.* 2019). Unlike *nia1 nia2* mutants, *nox1* mutants showed higher levels of NO during Cd treatment (Fig. 1). He *et al.* (2004) found that *nox1* mutants increase the NOS-l arginine substrate, suggesting that the arginine-dependent pathway is also involved in increasing NO production under Cd stress conditions in these mutants (Fig. 1 and Suppl. Fig. S2).

Interestingly, we observed a sharp decline in peroxule production in response to Cd in *px-ck* seedlings incubated with the NO scavenger cPTIO, and also in *nia1 nia2 x px-ck* seedlings, which produce less NO (Fig. 2B and 2C). The phenotype observed in *nia1 nia2 x px-ck* was restored when supplied with NO (Fig. 2C). Taken together, these data suggest that the signalling molecule NO, a positive regulator of peroxule production in plant responses to Cd stress, is involved in the complex network which regulates early responses to Cd. Although the energy costs of producing peroxules and the existence of different peroxisomal populations with specific functions may explain why an excess of NO does not increase the number of peroxule-producing peroxisomes, this issue needs further in-depth analysis. To our knowledge, peroxule production is associated with ROS production through exogenous applications of H_2O_2 (Sinclair *et al.* 2009; Barton, Mathur & Mathur 2013) and endogenous RBOH-dependent ROS

418 production in response to Cd stress (Rodríguez-Serrano *et al.* 2016). The molecular
419 events involved in peroxule extensions, such as the peroxine PEX11a, are not well
420 understood (Rodríguez-Serrano *et al.* 2016). PEX11a was found to be induced in WT
421 seedlings in response to Cd as described elsewhere (Rodríguez-Serrano *et al.* 2016),
422 although no changes in its expression were observed in the NO-related mutants; this
423 suggests that gene induction may not be necessary to produce peroxules and that redox-
424 dependent PTMs could be involved. In fact, the activation of yeast peroxine Pex11p
425 depends on redox changes in its cysteins (Knoblach & Rachubinski 2010; Schrader,
426 Bonekamp & Islinger 2012). Other PTMs can not be ruled out however, as PEX11a has
427 been identified as a putative target of phosphorylation in Arabidopsis (Kataya, Muench
428 & Moorhead 2019; Sandalio *et al.* 2019). Further proteomic analysis is required to
429 clarify the PTM dependence of PEX11a on the rapid regulation of peroxule formation
430 and the possible involvement of NO.

431 **NO regulation of peroxisome proliferation**

432 Peroxisome proliferation is associated with ROS accumulation and stress
433 (Lopez-Huertas, Charlton, Johnson, Graham & Baker 2000; Palma, Garrido, Rodríguez-
434 García & del Río 1991; Oksanen, Häikiö, Sober & Karnosky 2003; Nila, Sandalio,
435 López, del Rio & Gomez-Lim 2006; Castillo *et al.* 2008; Mitsuya *et al.* 2010),
436 particularly in plant responses to Cd (Romero-Puertas *et al.* 1999; Rodríguez-Serrano *et*
437 *al.* 2016; Calero-Muñoz *et al.* 2019). In this study, we show that NO regulates
438 peroxisome proliferation in response to Cd (Fig. 4A and B) and also appears to be a
439 positive regulator of peroxule production. Only phytochrome A (phy A), the bZIP
440 transcription factor HY5 homolog (HYH) and the peroxin PEX11b are involved in
441 upstream peroxisome proliferation signalling during seedling photo-morphogenesis
442 (Desai & Hu 2008). On the other hand, jasmonic acid (JA) appears to be a negative

443 regulator of peroxisome proliferation in Arabidopsis mesophyll cells (Castillo *et al.*
444 2008). The interesting antagonistic relationship that exists between NO and JA in
445 peroxisome proliferation requires further study in order to gain a deeper insight into the
446 mechanisms involved.

447 Interestingly, although peroxisome proliferation appears to be unaffected in
448 *nox1* x *px-ck* mutants, the number of peroxisomes per cell is always lower than in *px-ck*
449 mutants (Fig. 4C), which does not seem to be associated with *PEX11a* expression.
450 Peroxisome size and numbers were found to increase in potato treated with high
451 concentrations of JA (Ulloa, Raíces, MacIntosh, Maldonado & Téllez-Iñón 2002), while
452 the number of enlarged peroxisomes was found to decrease in Arabidopsis leaves
453 treated with JA (Castillo *et al.* 2008). Although the mechanisms involved in the
454 regulation of peroxisome proliferation and elongation under JA treatment conditions
455 remain unclear, they do not appear to depend on either *PEX11* or *DRP3A* (Castillo *et al.*
456 2008).

457 **NO regulation of ROS metabolism in peroxisomes**

458 We observed an increase in the number of peroxisomes containing precipitates
459 in *px-ck* after 3 h of Cd treatment (Fig. 5D and I), which could be associated with H_2O_2
460 and/or CAT activity (Romero-Puertas *et al.* 2004; Shibata *et al.* 2013). H_2O_2 has
461 previously been shown to increase in response to Cd stress in pea leaf peroxisomes
462 (Romero-Puertas *et al.* 1999) and in Arabidopsis seedlings expressing the H_2O_2
463 biosensor HyPer in peroxisomes (Calero-Muñoz *et al.* 2019). It is interesting to note
464 that these precipitates in *nia1 nia2 x px-ck* and especially in *nox1* x *px-ck* mutants were
465 observed under control conditions, suggesting that peroxisomal H_2O_2 metabolism is
466 altered in these mutants (Fig. 5B, C and I). Other organelles, such as mitochondria and
467 chloroplasts, have been reported to be affected in *nox1* mutants (Voll *et al.* 2003;

468 Hourton-Cabassa *et al.* 1998; Bona, Marsano, Cavaletto & Berta 2007; Voll *et al.* 2003;
469 Hu *et al.* 2014).

470 Interestingly, H_2O_2 content was found to decease significantly in both NO-
471 related mutants, a process which was maintained in *nia1 nia2* mutants (Fig. 6A),
472 although no changes were observed in WT. As described elsewhere, GST transcripts
473 were observed to increase after 3 h of Cd treatment (Calero-Muñoz et al. 2019), with a
474 similar result observed in mulberry plants (Xu et al. 2019). Although *nia1 nia2* mutants
475 behaved in a similar way to WT, no changes in GST expression were noted in *nox1*
476 seedlings (Fig. 6 B). This suggests that NO modifies H_2O_2 content and its dependent
477 signalling. The exogenous addition of NO donors is well known to increase antioxidant
478 activities such as GST after treatment with paraquat, As or Cd (Nahar *et al.* 2016;
479 Hasanuzzaman *et al.* 2018; Souri, Karimi, Farooq & Sandalio 2020), while an excess of
480 endogenous NO may inhibit antioxidant activity under Cd stress conditions (Terrón-
481 Camero et al. 2020).

482 The results obtained for CAT activity and *CAT2* expression, as well as protein
483 PTMs, in NO-related mutants as compared to WT show that peroxisomal oxidative
484 metabolism is regulated by NO. The decrease in CAT activity observed in WT under Cd
485 stress could be explained by its increased oxidation status. CAT has previously been
486 shown to be carbonylated and *S*-nitrosylated in pea plants in response to Cd, leading to
487 an inhibition in CAT activity (Romero-Puertas *et al.* 2002; Ortega-Galisteo *et al.* 2012),
488 while CAT is subject to oxidation in the presence of H_2O_2 in multiple sites (Nguyen &
489 Donaldson 2005; Anand, Kwak, Simha & Donaldson 2009). CAT activity was also
490 affected by increased NO and $O_2^{\cdot -}$ production in peroxisomes from Arabidopsis plants
491 treated with Pb (Corpas & Barroso 2017). Interestingly, CAT is more oxidized under
492 control conditions in *nia1 nia2* mutants than in WT; the oxidation status of CAT, unlike

493 in WT, was observed to decrease in both NO-related mutants in response to Cd,
494 probably due, in part, to the decrease observed in H_2O_2 content. *S*-nitrosylated CAT
495 activity increases under control conditions in NO-related mutants as compared to WT
496 seedlings, suggesting that CAT is protected from oxidation by *S*-nitrosylation.
497 Similarly, in sorghum leaves, salt stress promotes opposite patterns of carbonylation and
498 *S*-nitrosylation of C4 phosphoenolpyruvate carboxylase (PEPCase; Baena, Feria,
499 Echeverría, Monreal & García-Mauriño 2017); in addition, specific patterns of
500 carbonylation and *S*-nitrosylation under salt stress conditions are essential for citrus
501 plant vigour (Tanou *et al.* 2014). It has also been suggested that *S*-nitrosylation of
502 antioxidant enzymes prevents irreversible protein carbonylation during recalcitrant seed
503 desiccation tolerance in *Antiaris toxicaria* (Bai *et al.* 2011). Although CAT was more
504 oxidized and *S*-nitrosylated in *nia1 nia2* mutants under control conditions, an increase
505 in *CAT2* expression and protein content, and thus also in CAT activity, was observed.

506 **Peroxisome-dependent signalling in response to Cd is altered in NO-related**
507 **mutants**

508 ROS secondary messengers activate a signal transduction pathway culminating
509 in the regulation of gene expression, which is critical for plant subsistence (Foyer &
510 Noctor 2003; Suzuki, Shimazu & Tanaka 2012; Mittler 2017; Baxter *et al.* 2014).
511 Peroxisomal H_2O_2 induce transcripts, such as *FES1A* and the *HSP20-like* chaperone,
512 involved in protein repair responses, leading to stress tolerance and plant survival under
513 stressful conditions (Sewelam *et al.* 2014; Zhang *et al.* 2010). Both NO-related mutants
514 were found to affect very early responses to Cd, with *FES1A* and *HSP20-like* expression
515 observed to be significantly lower than in WT (Fig. 8). Both mutants showed a decrease
516 in H_2O_2 in response to Cd as compared to WT, which could explain the lower
517 expression of the repair genes. After three hours of Cd treatment, gene induction was

restored in *nia1 nia2* mutants in a manner similar to that in WT, while *nox1* mutants remained affected, suggesting that an excess of NO partly disrupts peroxisome-dependent signaling.

In summary, NO affects peroxisomal distribution, metabolism and dynamics, which impact organelle functionality and peroxisome-dependent signalling in plant responses to Cd stress (Fig. 9). The level of NO was observed to be lower in *nia1 nia2* mutants than in WT, which is essential for peroxule production and peroxisome proliferation. Peroxisomal oxidative metabolism is disturbed in NO-related mutants, with CAT being one of the antioxidants altered at the transcriptional and post-translational level. Peroxisome-dependent signalling in plant responses to Cd stress is also affected in NO-related mutants (Fig. 9). Although further research on the molecular mechanisms underlying the role of NO in peroxisomes is required, this study shows that NO needs to be tightly regulated in order to optimize peroxisome function and signalling.

Acknowledgements

This study was co-funded by the Spanish Ministry of Science, Innovation and Universities (MCIU), the State Research Agency (AEI) and the European Regional Development Fund (ERDF; PGC2018-098372-B-100 and BIO2015-67657-P). LC T-C was supported by a University Staff Training (FPU) fellowship from the Spanish Ministry of Education, Culture and Sports. Confocal laser fluorescence microscopic analyses were carried out at the Center for Scientific Instrumentation (CIC) of the University of Granada (UGR). We also wish to thank Angela Tate and Michael O'Shea for proofreading the English manuscript. None of the authors have any conflict of interest to declare.

Figure Legends

Figure 1: Effect of cadmium on NO accumulation in Arabidopsis seedlings.

Total NO content determined by DAF2-DA fluorescence under control (0 h) and Cd conditions in *nia1 nia2*, *nox1* and WT seedlings. Data are mean and standard errors (error bars) of at least three independent experiments. Different letters denote significant differences between Cd treatment time points within the same genotype (WT: lower case; *nia1 nia2*: upper case and *nox1*: italics), obtained using Tukey multiple comparison tests (p-value <0.05). Asterisks denote significant differences between *nia1 nia2* or *nox1* and WT within a time point according to the Student´s t-test (p-value < 0.05).

Figure 2: Effect of cadmium on peroxule formation in Arabidopsis seedlings.

(A) Representative images of peroxisomes (in green) under control conditions and after Cd treatment (30 min), producing peroxules (arrows). (B) Effect of cPTIO (0.5 mM), a NO scavenger, on peroxule formation induced in *px-ck* seedlings after Cd treatment (30 min.). (C) Peroxule formation in *px-ck, nia1 nia2 x px-ck* and *nox1* x *px-ck* seedlings after Cd treatment and effect of NO donor GSNO (0.5 mM) on peroxule formation in *px-ck* and *nia1 nia2 x px-ck* after Cd treatment (30 min.). Data are means, distributions and whiskers (maximum and minimum) of at least three independent experiments. Different letters denote significant differences between different treatments according to the Student´s t-test (p-value < 0.05) in (B); and between different treatments and genotypes according to the Tukey multiple comparison tests (p-value <0.05) in (C).

Figure 3: Effect of cadmium on *PEX11a* expression in Arabidopsis seedlings.

Time course analysis of *PEX11a* expression by qRT-PCR under control (0 h) and Cd conditions in *nia1 nia2*, *nox1* and WT seedlings. Data are mean and standard errors (error bars) of at least three independent experiments. Different letters denote significant differences between Cd treatment time points within the same genotype obtained using

Tukey multiple comparison tests (p-value <0.05). The absence of letters denote no significant changes within the genotype following Cd treatment. Asterisks denote significant differences between *nia1 nia2* or *nox1* and WT within a time point according to the Student´s t-test (p-value < 0.05).

Figure 4: Effect of cadmium on peroxisome proliferation.

(A) Number of peroxisomes per cell slice under control conditions and after Cd treatment (3 h) in *nia1 nia2* x *px-ck*, *nox1* x *px-ck* and *px-ck* seedlings, analysed by cytochemistry and optical microscopy (from thin leaf sections shown in Suppl. Fig. S5). (B) Quantification of peroxisome accumulation analysed by the marker protein peroxin 14 (PEX14) in WT, *nox1*, and *nia1 nia2* after Cd treatment (3 h) and *nia1 nia2* supplemented with the NO donor, GSNO (0.5 mM). (C) Distribution of peroxisomes by number of these organelles in each cell slice analysed by cytochemistry and optical microscopy. The percentage of cells containing from 1 to 10 peroxisomes is shown. Data represent distribution and whiskers (maximum and minimum) in A), and mean and standard error (error bars) in B) and C), of at least three independent experiments. In A) and C), different letters denote significant differences between Cd treatment and control within the same genotype according to the Student´s t-test (p-value < 0.05). Asterisks denote significant differences between *nia1 nia2 x px-ck* or *nox1* x *px-ck* and *px-ck* within a time point according to the Student´s t-test (p-value < 0.05). In B), asterisks denote significant differences between Cd or Cd+GSNO treatments and control within the same genotype according to the Student´s t-test (p-value < 0.05); and the letter denotes significant differences between Cd+GSNO and Cd treatments in *nia1 nia2* mutants according to the Student´s t-test (p-value < 0.05).

Figure 5: Peroxisome ultrastructure in Arabidopsis seedlings under control and Cd treatment conditions.

Representative micrographs of leaf sections from *px-ck*, *nia1 nia2 x px-ck* and *nox1* x *px-ck* seedlings, treated (D, E, F) or not (A, B, C) with Cd (3 h), analyzed by electron microscopy (scale bar 1 µm). (G) Area, (H) circularity and (I) percentage of peroxisomes with precipitates. At least 600 cells were analyzed per treatment, meaning that thousands of peroxisomes were examined. Data are mean and standard error (error bars) of at least three independent experiments. Different letters denote significant differences between Cd treatment and control within the same genotype (*px-ck*: lower case; *nia1 nia2* x *px-ck*: upper case and *nox1* x *px-ck*: italics), obtained using the Student´s t-test (p-value <0.05). Asterisks denote significant differences between *nia1 nia2 x px-ck* or *nox1* x *px-ck* and *px-ck* within a time point according to the Student´s t-test (p-value < 0.05). Abbreviations: ch, chloroplasts; m, mitochondria; p, peroxisome; v, vacuole; s, starch. Arrows indicate precipitates inside the peroxisomes.

Figure 6: H_2O_2 metabolism in Arabidopsis seedlings under Cd stress.

(A) H_2O_2 content determined by fluorimetry, (B) expression of *GST* by qRT-PCR (C) catalase activity and (E) *CAT2* expression by qR-TPCR in WT, *nia1nia* and *nox1* seedlings under Cd treatment (0-3 h). Data are mean and standard error (error bars) of at least three independent experiments. Different letters denote significant differences between time points of Cd treatment within the same genotype (WT: lower-case; *nia1 nia2*: upper case and *nox1*: italics), obtained by Tukey multiple comparison tests (p-value <0.05). The absence of letters denote no significant differences within the genotype following Cd treatment. Asterisks denote significant differences between *nia1 nia2* or *nox1* and WT within a time point according to the Student´s t-test (p-value < 0.05).

Figure 7: Effect of cadmium on catalase post-transcriptional modifications in Arabidopsis seedlings.

(A) Representative Western blot with oxidation pattern of CAT following Cd treatment (30 min.) in WT, *nia1 nia2* and *nox1* seedlings and quantification. Protein extracts from seedlings were subjected to derivatization with DNPH, immunoprecipitated with anti-DNPH (oxidized proteins) and CAT was then identified by a specific antibody. Non-derivatized samples from *nia1 nia2* were used as negative control. (B) Representative Western blot with *S*-nitrosylation pattern of CAT following Cd treatment (30 min.) in WT, *nia1 nia2* and *nox1* seedlings and quantification. Protein extracts from seedlings were subjected to the biotin-switch method. *S*-nitrosylated proteins were then purified by an anti-biotin antibody and subjected to Western blot analysis with an anti-CAT antibody. Non-biotinylated samples from *nia1 nia2* were used as negative control. Data represent mean and standard error (error bars) of at least three independent experiments. Different letters (WT: lower-case; *nia1 nia2*: upper case and *nox1*: italics) denote significant differences between Cd treatment and control within the same genotype according to the Student´s t-test (p-value < 0.05). The absence of letters mean no significant differences with Cd treatment within a genotype. Asterisks denote significant differences between *nia1 nia2* or *nox1* and WT within a time point according to the Student´s t-test (p-value < 0.05).

Figure 8: Effect of cadmium on *HSP20*-like and *FES1A* gene expression. *HSP20-like* (A) and *FES1A* (B) gene expression by qRT-PCR in WT, *nia1 nia2* and *nox1*seedlings under Cd treatment (0-3 h). Data represent mean and standard error (error bars) of at least three independent experiments. Different letters denote significant differences between Cd treatment time points within the same genotype (WT: lower-case; *nia1 nia2*: upper case and *nox1*: italics), obtained using Tukey multiple comparison tests (p-value <0.05). Asterisks denote significant differences between *nia1*

642 *nia2* or *nox1* and WT within a time point according to the Student´s t-test (p-value <
643 0.05).

644 **Figure 9: Model for NO function in peroxisomal dynamics in the early plant**
645 **response to Cd treatment.**

646 Cd induces ROS and NO production, with *nia1 nia2* mutants showing lower overall
647 levels of NO. Thus, peroxule production and peroxisome proliferation in *nia1 nia2*
648 mutants, whose phenotype is restored by addition of NO. Altered levels of NO
649 following Cd treatment (30 min) partly inhibit peroxisome-dependent signalling, which
650 is inhibited by an excess of NO after 3h. Peroxisomal ROS metabolism is also altered in
651 NO-related mutants, with CAT levels and activity found to be higher in *nia1 nia2*
652 mutants than in WT plants.

654 **References**

655 Aebi H. (1984) Catalase in vitro. *Methods in enzymology* **105**, 121-126.

656 Anand P., Kwak Y., Simha R. & Donaldson R.P. (2009) Hydrogen peroxide induced
657 oxidation of peroxisomal malate synthase and catalase. *Archives of Biochemistry and*
658 *Biophysics* **491**, 25-31.

659 Baena G., Feria A.B., Echeverría C., Monreal J.A. & García-Mauriño S. (2017) Salinity
660 promotes opposite patterns of carbonylation and nitrosylation of C4
661 phosphoenolpyruvate carboxylase in sorghum leaves. *Planta* **246**, 1203-1214.

662 Bai X., Yang L., Tian M., Chen J., Shi J., Yang Y. & Hu X. (2011) Nitric oxide
663 enhances desiccation tolerance of recalcitrant *Pseudomonas antiaris* toxicaria seeds via
664 protein *S*-nitrosylation and carbonylation. *PloS one* **6**, e20714.

665 Baker A. & Paudyal R. (2014) The life of the peroxisome: From birth to death. *Current*
666 *Opinion in Plant Biology* **22**, 39-47.

667 Bartha B., Kolbert Z. & Erdei L. (2005) Nitric oxide production induced by heavy
668 metals in *Brassica juncea* L. Czern and *Pisum sativum* L. *Acta Biologica Szegediensis*
669 **49**, 9-12.

670 Barton K., Mathur N. & Mathur J. (2013) Simultaneous live-imaging of peroxisomes
671 and the ER in plant cells suggests contiguity but no luminal continuity between the two
672 organelles. *Frontiers in Physiology* **4**, 196.

673 Baxter A., Mittler N., Suzuky N. (2014) , ROS as key players in plant stress signalling
674 *Journal Experimental of Botany* **65**, 1229-1240.

675 Besson-Bard A., Gravot A., Richaud P., Auroy P., Duc C., Gaymard F., …
676 Wendehenne D. (2009) Nitric oxide contributes to cadmium toxicity in Arabidopsis by
677 promoting cadmium accumulation in roots and by up-regulating genes related to iron
678 uptake. *Plant physiology* **149**, 1302-1315.

679 Bona E., Marsano F., Cavaletto M. & Berta G. (2007) Proteomic characterization of
680 copper stress response in *Cannabis sativa* roots. *Proteomics* **7**, 1121-1130.

681 Calero-Muñoz N., Exposito-Rodríguez M., Collado-Arenal A.M., Rodríguez-Serrano
682 M., Laureano-Marín A.M., Santamaría M.E., … Sandalio L.M. (2019) Cadmium
683 induces Reactive Oxygen Species-dependent pexophagy in Arabidopsis leaves. *Plant,*
684 *Cell & Environment* **42**, 2696-2714.

685 Castillo M.C., Coego A., Costa-Broseta Á. & León J. (2018) Nitric oxide responses in
686 Arabidopsis hypocotyls are mediated by diverse phytohormone pathways. *Journal of*
687 *Experimental Botany* **69**, 5265-5278.

688 Castillo M.C., Sandalio L.M., del Río L.A. & León J. (2008) Peroxisome proliferation,
689 wound-activated responses and expression of peroxisome-associated genes are cross-
690 regulated but uncoupled in *Arabidopsis thaliana*. *Plant, Cell & Environment* **31**, 492-
691 505.

692 Chen W.W., Jin J.F., Lou H.Q., Liu L., Kochian L. V. & Yang J.L. (2018) LeSPL-CNR
693 negatively regulates Cd acquisition through repressing nitrate reductase-mediated nitric
694 oxide production in tomato. *Planta* **248**, 893-907.

695 Corpas F.J. & Barroso J.B. (2017) Lead-induced stress, which triggers the production of
696 nitric oxide (NO) and superoxide anion ($O_2^{\cdot-}$) in Arabidopsis peroxisomes, affects
697 catalase activity. *Nitric Oxide* **68**, 103-110.

698 Desai M. & Hu J. (2008) Light induces peroxisome proliferation in Arabidopsis
699 seedlings through the photoreceptor phytochrome A, the transcription factor HY5
700 HOMOLOG, and the peroxisomal protein PEROXIN11b. *Plant physiology* **146**, 1117-
701 1127.

702 Desikan R., Griffiths R., Hancock J. & Neill S. (2002) A new role for an old enzyme:
703 Nitrate reductase-mediated nitric oxide generation is required for abscisic acid-induced
704 stomatal closure in *Arabidopsis thaliana*. *Proceedings of the National Academy of*
705 *Sciences* **99**, 16314-16318.

706 Foyer C.H. & Noctor G. (2003) Redox sensing and signalling associated with reactive
707 oxygen in chloroplasts, peroxisomes and mitochondria. *Physiologia Plantarum* **119**,
708 355-364.

709 Fransen M., Lismont C. & Walton P. (2017) The Peroxisome-mitochondria connection:
710 How and why? *International Journal of Molecular Sciences* **18**, 1126.

711 Groppa M.D., Zawoznik M.S., Tomaro M.L. & Benavides M.P. (2008) Inhibition of
712 root growth and polyamine metabolism in sunflower (*Helianthus annuus*) seedlings
713 under cadmium and copper stress. *Biological Trace Element Research* **126**, 246-256.

714 Guo F.Q., Okamoto M. & Crawford N.M. (2003) Identification of a plant nitric oxide
715 synthase gene involved in hormonal signaling. *Science* **302**, 100-103.

716 Gupta D.K. & Sandalio L.M. (2012) *Metal toxicity in plants : perception, signaling and*
717 *remediation*. Springer.

718 Hasanuzzaman M., Nahar K., Rahman A., Mahmud J. Al, Alharby H.F. & Fujita M.
719 (2018) Exogenous glutathione attenuates lead-induced oxidative stress in wheat by

720 improving antioxidant defense and physiological mechanisms. *Journal of Plant*
721 *Interactions* **13**, 203-212.

722 He Y., Tang R.H., Hao Y., Stevens R.D., Cook C.W., Ahn S.M., … Pei Z.-M. (2004)
723 Nitric Oxide Represses the Arabidopsis Floral Transition. *Science* **305**, 1968-1971.

724 Hoagland D.R. & Arnon D.I. (1950) The water-culture method for growing plants
725 without soil. *Circular. California Agricultural Experiment Station* **347**, 31.

726 Hourton-Cabassa C., Ambard-Bretteville F., Moreau F., Davy de Virville J., Remy R. &
727 Francs-Small C.C. (1998) Stress induction of mitochondrial formate dehydrogenase in
728 potato leaves. *Plant Physiologyhysiology* **116**, 627-635.

729 Hu J., Baker A., Linka N., Mullen R., Reumann S. & Zoman B. (2012) Plant
730 peroxisomes: Biogenesis and function. *The Plant Cell* **24**, 2279-2303.

731 Hu W.J., Chen J., Liu T.W., Liu X., Chen J., Wu F.H., … Zheng H.L. (2014)
732 Comparative proteomic analysis on wild type and nitric oxide-overproducing mutant
733 (*nox1*) of *Arabidopsis thaliana*. *Nitric Oxide* **36**, 19-30.

734 Kao Y.T., Gonzalez K.L. & Bartel B. (2018) Update on plant peroxisomes peroxisome
735 function, biogenesis, and dynamics in plants. *Plant Physiology* **176**, 162-177.

736 Kataya A.R.A., Muench D.G. & Moorhead G.B. (2019) A framework to investigate
737 peroxisomal protein phosphorylation in Arabidopsis. *Trends in Plant Science* **24**, 366-
738 381.

739 Knoblach B. & Rachubinski R.A. (2010) Phosphorylation-dependent activation of
740 peroxisome proliferator protein PEX11 controls peroxisome abundance. *Journal of*
741 *Biological Chemistry* **285**, 6670-6680.

742 Kovacs I. & Lindermayr C. (2013) Nitric oxide-based protein modification: formation
743 and site-specificity of protein *S*-nitrosylation. *Frontiers in Plant Science* **4**, 1-10.

744 León J., Costa Á. & Castillo M.-C. (2016) Nitric oxide triggers a transient metabolic
745 reprogramming in Arabidopsis. *Scientific Reports* **6**, 37945.

746 Lindermayr C. & Durner J. (2015) Interplay of reactive oxygen species and nitric oxide:
747 nitric oxide coordinates reactive oxygen species homeostasis. *Plant Physiology* **167**,
748 1209-1210.

749 Lopez-Huertas E., Charlton W.L., Johnson B., Graham I.A. & Baker A. (2000) Stress
750 induces peroxisome biogenesis genes. *The EMBO Journal* **19**, 6770.

751 Lozano-Juste J. & Leon J. (2010) Enhanced abscisic acid-mediated responses in *nia1*
752 *nia2noa1-2* triple mutant impaired in *NIA/NR*- and *AtNOA1*-dependent nitric oxide
753 biosynthesis in Arabidopsis. *Plant Physiology* **152**, 891-903.

754 Marinho H.S., Real C., Cyrne L., Soares H. & Antunes F. (2014) Hydrogen peroxide
755 sensing, signaling and regulation of transcription factors. *Redox Biology* **2**, 535-562.

756 Martínez-Ruiz A., Cadenas S. & Lamas S. (2011) Nitric oxide signaling: Classical, less
757 classical, and nonclassical mechanisms. *Free Radical Biology and Medicine* **51**, 17-29.

758 Mathur J., Shaikh A. & Mathur N. (2018) Peroxisome mitochondria inter-relations in
759 plants. In *Proteomics of Peroxisomes*, Springer. (eds L.A. del Río & M. Schrader), pp.
760 417-433. Springer, Singapore.

761 Mitsuya S., El-Shami M., Sparkes I.A., Charlton W.L., Lousa C.D.M., Johnson B. &
762 Baker A. (2010) Salt stress causes peroxisome proliferation, but inducing peroxisome

763 proliferation does not improve NaCl tolerance in *Arabidopsis thaliana*. *PloS one* **5**,
764 e9408.

765 Mittler R. (2017) ROS Are Good. *Trends in Plant Science* **22**, 11-19.

766 Modolo L. V., Augusto O., Almeida I.M.G., Magalhaes J.R. & Salgado I. (2005) Nitrite
767 as the major source of nitric oxide production by *Arabidopsis thaliana* in response to
768 *Pseudomonas syringae*. *FEBS Letters* **579**, 3814-3820.

769 Moreau M., Lee G.I., Wang Y., Crane B.R. & Klessig D.F. (2008) *AtNOS/AtNOA1* is a
770 functional *Arabidopsis thaliana* cGTPase and not a nitric-oxide synthase. *The Journal*
771 *of biological chemistry* **283**, 32957-67.

772 Nahar K., Hasanuzzaman M., Alam M.M., Rahman A., Suzuki T. & Fujita M. (2016)
773 Polyamine and nitric oxide crosstalk: Antagonistic effects on cadmium toxicity in mung
774 bean plants through upregulating the metal detoxification, antioxidant defense and
775 methylglyoxal detoxification systems. *Ecotoxicology and Environmental Safety* **126**,
776 245-255.

777 Nakatsubo N., Kojima H., Kikuchi K., Nagoshi H., Hirata Y., Maeda D., … Nagano T.
778 (1998) Direct evidence of nitric oxide production from bovine aortic endothelial cells
779 using new fluorescence indicators: diaminofluoresceins. *FEBS Letters* **427**, 263-266.

780 Nelson B.K., Cai X. & Nebenführ A. (2007) A multicolored set of in vivo organelle
781 markers for co-localization studies in Arabidopsis and other plants. *The Plant Journal :*
782 *for Cell and Molecular Biology* **51**, 1126-1136.

783 Nguyen A.T. & Donaldson R.P. (2005) Metal-catalyzed oxidation induces
784 carbonylation of peroxisomal proteins and loss of enzymatic activities. *Archives of*
785 *Biochemistry and Biophysics* **439**, 25-31.

786 Nila A.G., Sandalio L.M., López M.G., del Rio M.G. & Gomez-Lim M.A. (2006)
787 Expression of a peroxisome proliferator-activated receptor gene (xPPAR) from *Xenopus*
788 *laevis* in tobacco (*Nicotiana tabacum*) plants. *Planta* **224**, 569-581.

789 Oksanen E., Häikiö E., Sober J. & Karnosky D.F. (2003) Ozone-induced H_2O_2
790 accumulation in field-grown aspen and birch is linked to foliar ultrastructure and
791 peroxisomal activity. *New Phytologist.* **161**, 791-799.

792 Ortega-Galisteo A.P., Rodríguez-Serrano M., Pazmiño D.M., Gupta D.K., Sandalio
793 L.M. & Romero-Puertas M.C. (2012) *S*-Nitrosylated proteins in pea (*Pisum sativum* L.)
794 leaf peroxisomes: Changes under abiotic stress. *Journal of Experimental Botany* **63**,
795 2089-103.

796 Palma J., Garrido M., Rodríguez-García M.I. & del Río L.A. (1991) Peroxisome
797 proliferation and oxidative stress mediated by activated oxygen species in plant
798 peroxisomes. *Archives of Biochemistry and Biophysics* **287**, 68-74.

799 Pérez-Chaca M.V., Rodríguez-Serrano M., Molina A.S., Pedranzani H.E., Zirulnik F.,
800 Sandalio L.M. & Romero-Puertas M.C. (2014) Cadmium induces two waves of reactive
801 oxygen species in *Glycine max*(L.) roots. *Plant, Cell & Environment* **37**, 1672-1687.

802 Pfaffl M.W. (2001) A new mathematical model for relative quantification in real-time
803 RT-PCR. *Nucleic acids research* **29**, e45.

804 Remans T., Keunen E., Bex G.J., Smeets K., Vangronsveld J. & Cuypers A. (2014)
805 Reliable gene expression analysis by reverse transcription-quantitative PCR: Reporting
806 and minimizing the uncertainty in data accuracy. *The Plant Cell* **26**, 3829-3837.

807 Reumann S. & Bartel B. (2016) Plant peroxisomes: recent discoveries in functional
808 complexity, organelle homeostasis, and morphological dynamics. *Current Opinion in*
809 *Plant Biology* **34**, 17-26.

810 Rockel P., Strube F., Rockel A., Wildt J. & Kaiser W.M. (2002) Regulation of nitric
811 oxide (NO) production by plant nitrate reductase in vivo and in vitro. *Journal of*
812 *Experimental Botany* **53**, 103-110.

813 Rodríguez-Serrano M., Romero-Puertas M.C., Pazmino D.M., Testillano P.S., Risueno
814 M.C., del Rio L.A. & Sandalio L.M. (2009) Cellular. *Plant Physiology* **150**, 229-243.

815 Rodríguez-Serrano M., Romero-Puertas M.C., Sanz-Fernández M., Hu J. & Sandalio
816 L.M. (2016) Peroxisomes extend peroxules in a fast response to stress via a reactive
817 oxygen species-mediated induction of the peroxin PEX11a. *Plant Physiology* **171**,
818 1665-1674.

819 Rodríguez-Serrano M., Romero-Puertas M.C., Sparkes I., Hawes C., del Río L.A. &
820 Sandalio L.M. (2009) Peroxisome dynamics in Arabidopsis plants under oxidative
821 stress induced by cadmium. *Free Radical Biology and Medicine* **47**, 1632-1639.

822 Romero-Puertas M.C., Laxa M., Matte A., Zaninotto F., Finkemeier I., Jones A.M.E.,
823 … Delledonne M. (2007) *S*-Nitrosylation of peroxiredoxin II E promotes peroxynitrite-
824 mediated tyrosine nitration. *The Plant cell Online* **19**, 4120-4130.

825 Romero-Puertas M.C., McCarthy I., Sandalio L.M., Palma J.M., Corpas F.J., Gómez M.
826 & del Río L.A. (1999) Cadmium toxicity and oxidative metabolism of pea leaf
827 peroxisomes. *Free radical research* **31 Suppl**, S25-31.

828 Romero-Puertas M.C., Palma J.M., Gómez M., Del Río L.A. & Sandalio L.M. (2002)
829 Cadmium causes the oxidative modification of proteins in pea plants. *Plant, Cell &*
830 *Environment* **25**, 677-686.

831 Romero-Puertas M.C., Rodríguez-Serrano M., Corpas F.J., Gómez M., Del Río L.A. &
832 Sandalio L.M. (2004) Cadmium-induced subcellular accumulation of $O_2^{\cdot-}$ and H_2O_2 in
833 pea leaves. *Plant, Cell & Environment* **27**, 1122-1134.

834 Romero-Puertas M.C. & Sandalio L.M. (2016) Role of NO-dependent posttranslational
835 modifications in switching metabolic pathways. *Advances in Botanical Research* **77**,
836 123-144.

837 Romero-Puertas M.C., Terrón-Camero L.C., Peláez-Vico M.A., Olmedilla A. &
838 Sandalio L.M. (2019) Reactive oxygen and nitrogen species as key indicators of plant
839 responses to Cd stress. *Enviromental and Experimental Botany* **161,** 107-119.

840 Sandalio L.M., Gotor C., Romero L.C. & Romero-Puertas M.C. (2019) Multilevel
841 regulation of peroxisomal proteome by post-translational modifications. *International*
842 *Journal of Molecular Sciences* **20**, 4881.

843 Sandalio L.M. & Romero-Puertas M.C. (2015) Peroxisomes sense and respond to
844 environmental cues by regulating ROS and RNS signalling networks. *Annals of Botany*
845 **116**, 475-485.

846 Sanz L., Albertos P., Mateos I., Sánchez-Vicente I., Lechón T., Fernández-Marcos M.
847 & Lorenzo O. (2015) Nitric oxide (NO) and phytohormones crosstalk during early plant
848 development. *Journal of Experimental Botany* **66**, 2857-2868.

849 Schrader M., Bonekamp N.A. & Islinger M. (2012) Fission and proliferation of
850 peroxisomes. *Biochimica et Biophysica Acta (BBA) - Molecular Basis of Disease* **1822**,
851 1343-1357.

852 Sewelam N., Jaspert N., Van Der Kelen K., Tognetti V.B., Schmitz J., Frerigmann H.,
853 … Maurino V.G. (2014) Spatial H_2O_2 Signaling specificity: H_2O_2 from chloroplasts and
854 peroxisomes modulates the plant transcriptome differentially. *Molecular Plant* **7**, 1191-
855 1210.

856 Shibata M., Oikawa K., Yoshimoto K., Kondo M., Mano S., Yamada K., … Nishimura
857 M. (2013) Highly oxidized peroxisomes are selectively degraded via autophagy in
858 *Arabidopsis*. *The Plant Cell* **25**, 4967-4983.

859 Sinclair A.M., Trobacher C.P., Mathur N., Greenwood J.S. & Mathur J. (2009) Peroxule
860 extension over ER-defined paths constitutes a rapid subcellular response to hydroxyl
861 stress. *The Plant Journal* **59**, 231-242.

862 Souri Z., Karimi N., Farooq M.A. & Sandalio L.M. (2020) Nitric oxide improves
863 tolerance to arsenic stress in *Isatis cappadocica* desv. Shoots by enhancing antioxidant
864 defenses. *Chemosphere* **239**, 124523.

865 Streatfield S.J., Weber A., Kinsman E.A., Häusler R.E., Li J., Post-Beittenmiller D., …
866 Chory J. (1999) The phosphoenolpyruvate/phosphate translocator is required for
867 phenolic metabolism, palisade cell development, and plastid-dependent nuclear gene
868 expression. *The Plant cell* **11**, 1609-1622.

869 Suzuki G., Shimazu N. & Tanaka M. (2012) A Yeast Prion, Mod5, Promotes acquired
870 drug resistance and cell survival under environmental stress. *Science* **336**, 355-359.

871 Tanou G., Ziogas V., Belghazi M., Christou A., Filippou P., Job D., … Molassiotis A.
872 (2014) Polyamines reprogram oxidative and nitrosative status and the proteome of citrus
873 plants exposed to salinity stress. *Plant, Cell & Environment* **37**, 864-885.

874 Terrón-Camero L.C., Molina-Moya E., Sanz-Fernández M., Sandalio L.M. & Romero-
875 Puertas M.C. (2018) Detection of reactive oxygen and nitrogen species (ROS/RNS)
876 during hypersensitive cell death. *Methods in Molecular Biology*. **1743**, 97-105.

877 Terrón-Camero L.C., Peláez-Vico M.A., Del Val C., Sandalio L.M. & Romero-Puertas
878 M.C. (2019) Role of nitric oxide in plant responses to heavy metal stress: Protection vs
879 toxicity. *Journal of Experimental Botany* **70**, 4477-4488.

880 Terrón-Camero L.C., Del Val C., Sandalio L.M. & Romero-Puertas M.C. (2020) Low
881 endogenous NO levels in roots and antioxidant systems are determinants for the
882 resistance of Arabidopsis seedlings grown in Cd. *Enviromental Polution* **256**, 113411

883 Ulloa R.M., Raíces M., MacIntosh G.C., Maldonado S. & Téllez-Iñón M.T. (2002)
884 Jasmonic acid affects plant morphology and calcium-dependent protein kinase
885 expression and activity in *Solanum tuberosum*. *Physiologia plantarum* **115**, 417-427.

886 Voll L., Hausler R.E., Hecker R., Weber A., Weissenbock G., Fiene G., … Flugge U.I.
887 (2003) The phenotype of the Arabidopsis *cue1* mutant is not simply caused by a general
888 restriction of the shikimate pathway. *The Plant Journal* **36**, 301-317.

889 Wilkinson J.Q. & Crawford N.M. (1993) Identification and characterization of a
890 chlorate-resistant mutant of *Arabidopsis thaliana* with mutations in both nitrate
891 reductase structural genes NIA1 and NIA2. *Molecular and General Genetics MGG* **239**,
892 289-297.

893 Xu Z., Dong M., Peng X., Ku W., Zhao Y. & Yang G. (2019) New insight into the
894 molecular basis of cadmium stress responses of wild paper mulberry plant by
895 transcriptome analysis. *Ecotoxicology and Environmental Safety* **171**, 301-312.

896 Yamasaki H. & Sakihama Y. (2000) Simultaneous production of nitric oxide and
897 peroxynitrite by plant nitrate reductase: In vitro evidence for the NR-dependent
898 formation of active nitrogen species. *Federation of European Biochemical Societies*
899 *letters* **468**, 89-92.

900 Yu M., Lamattina L., Spoel S.H. & Loake G.J. (2014) Nitric oxide function in plant
901 biology: A redox cue in deconvolution. *New Phytologist* **202**, 1142-1156.

902 Yun B.W., Spoel S.H. & Loake G.J. (2012) Synthesis of and signalling by small, redox
903 active molecules in the plant immune response. *Biochimica et Biophysica Acta (BBA) -*
904 General Subjects 1820, 770-776.

905 Zhang J.X., Wang C., Yang C.Y., Wang J.Y., Chen L., Bao X.M., … Liu J. (2010) The
906 role of Arabidopsis AtFes1A in cytosolic Hsp70 stability and abiotic stress tolerance.
907 The Plant Journal 62, 539-548.

A tight regulation of NO is required for optimal peroxisomal function and dependent signalling. NO is essential for peroxule production and peroxisome proliferation occurring in plant response to Cd. Additionally, peroxisome number and distribution as well as the oxidative metabolism of the organelle are altered by different levels of NO under control and stress conditions.

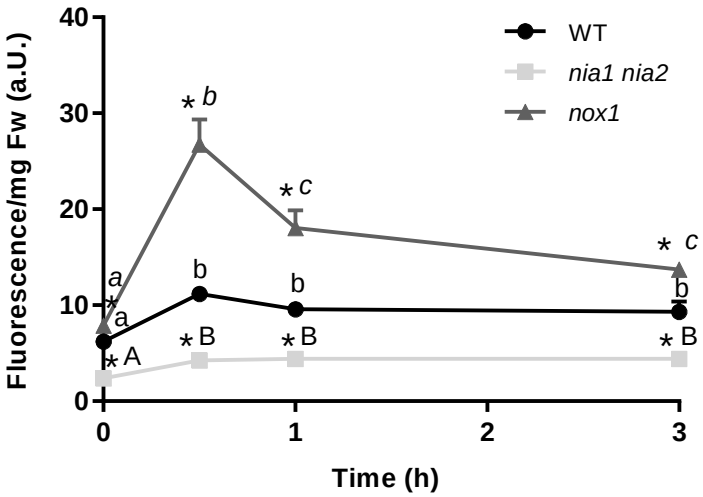
Fluorescence/mg Fw (a.U.)
40
30
20
10
0
0
1
2
3
Time (h)
WT
nia1 nia2
nox1
* b
* c
* c
a
* a
b
b
b
* A
* B
* B
* B

Figure 1

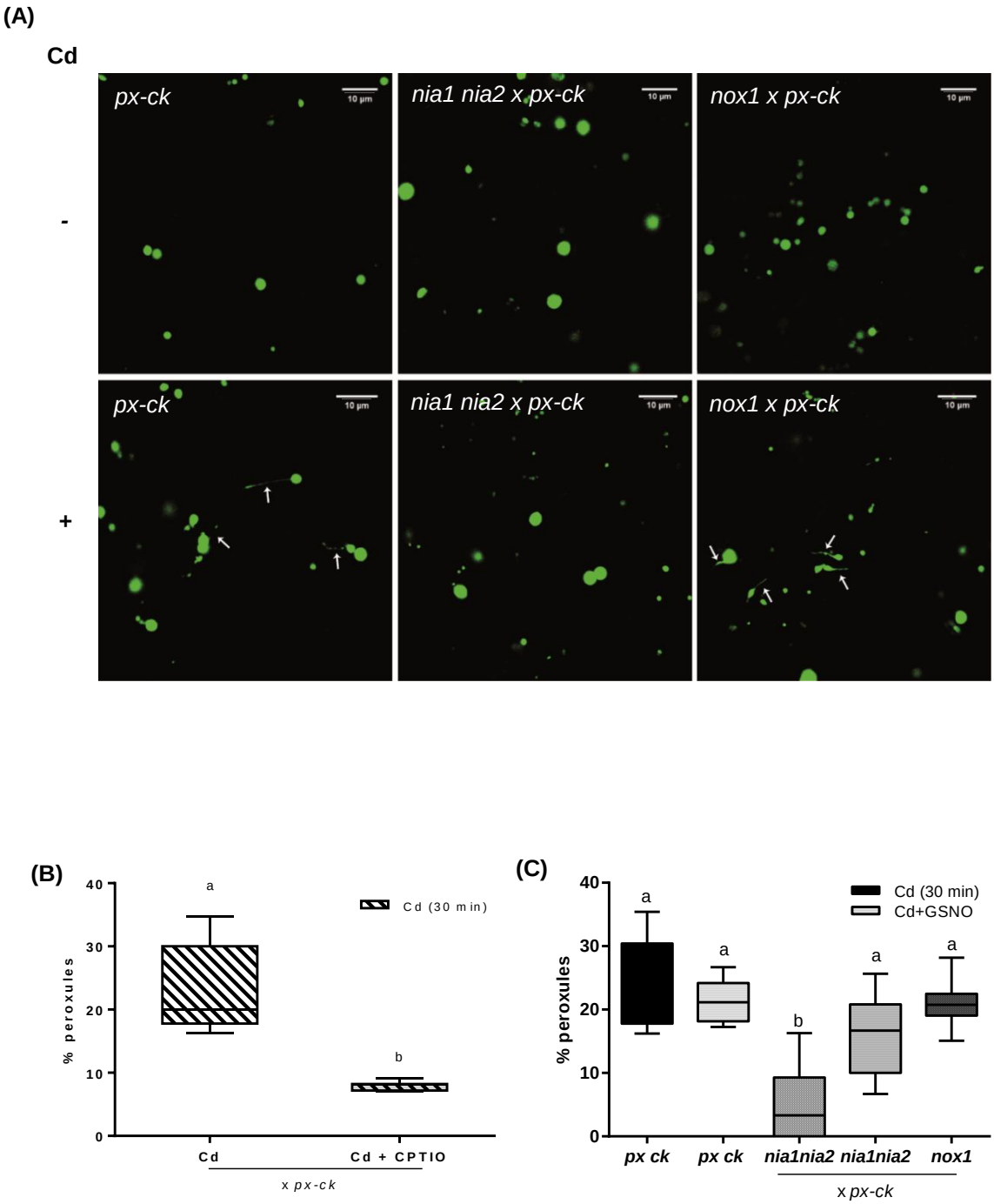
(A)
Cd
-
+
px-ck
nia1 nia2 x px-ck
nox1 x px-ck
10 µm
(B)
% peroxules
Cd (30 min)
Cd
Cd + CPTIO
x px-ck
(C)
% peroxules
Cd (30 min)
Cd+GSNO
px ck
px ck
nia1nia2
nia1nia2
nox1
x px-ck

Figure 2

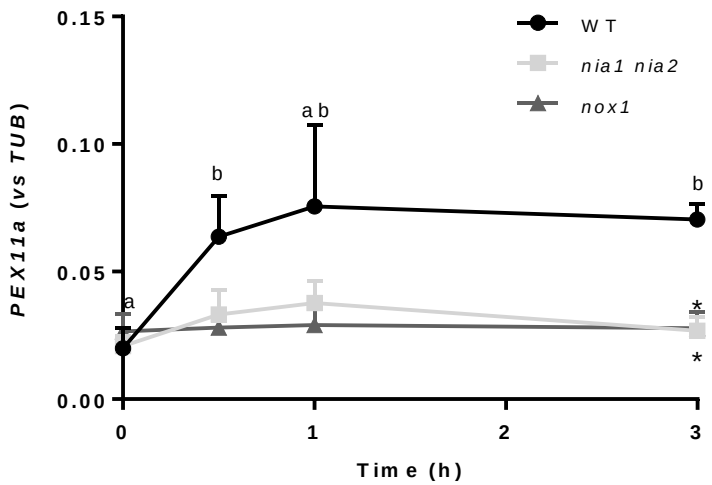
0.15
0.10
0.05
0.00
PEX11a (vs TUB)
0
1
2
3
Time (h)
WT
nia1 nia2
nox1
a
b
a b
b
*
*

Figure 3

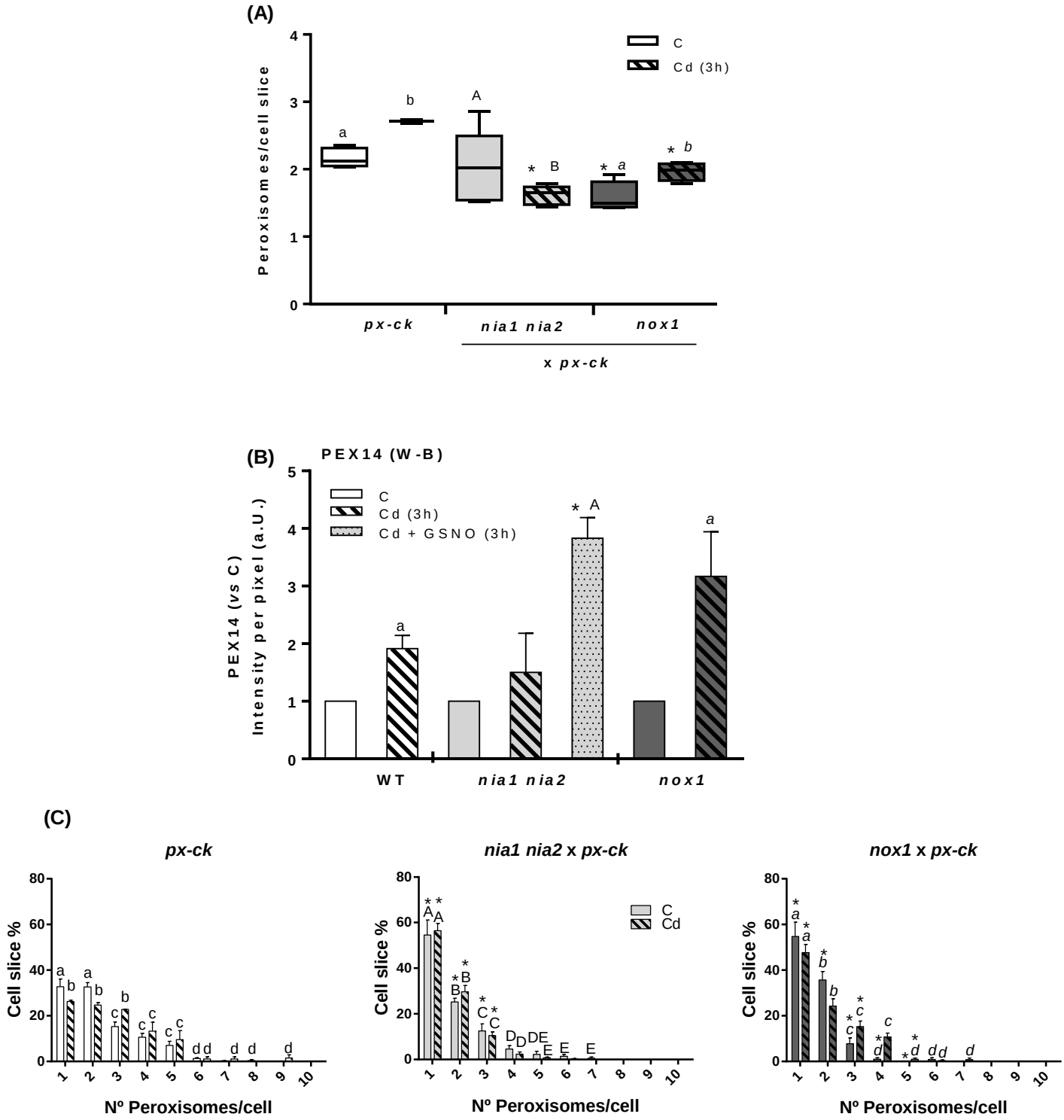
(A)
Peroxisomes/cell slice
C
Cd (3h)
px-ck
nia1 nia2
nox1
x px-ck
(B)
PEX14 (W-B)
PEX14 (vs C)
Intensity per pixel (a.U.)
C
Cd (3h)
Cd + GSNO (3h)
WT
nia1 nia2
nox1
(C)
px-ck
nia1 nia2 x px-ck
nox1 x px-ck
Cell slice %
Nº Peroxisomes/cell
C
Cd

Figure 4

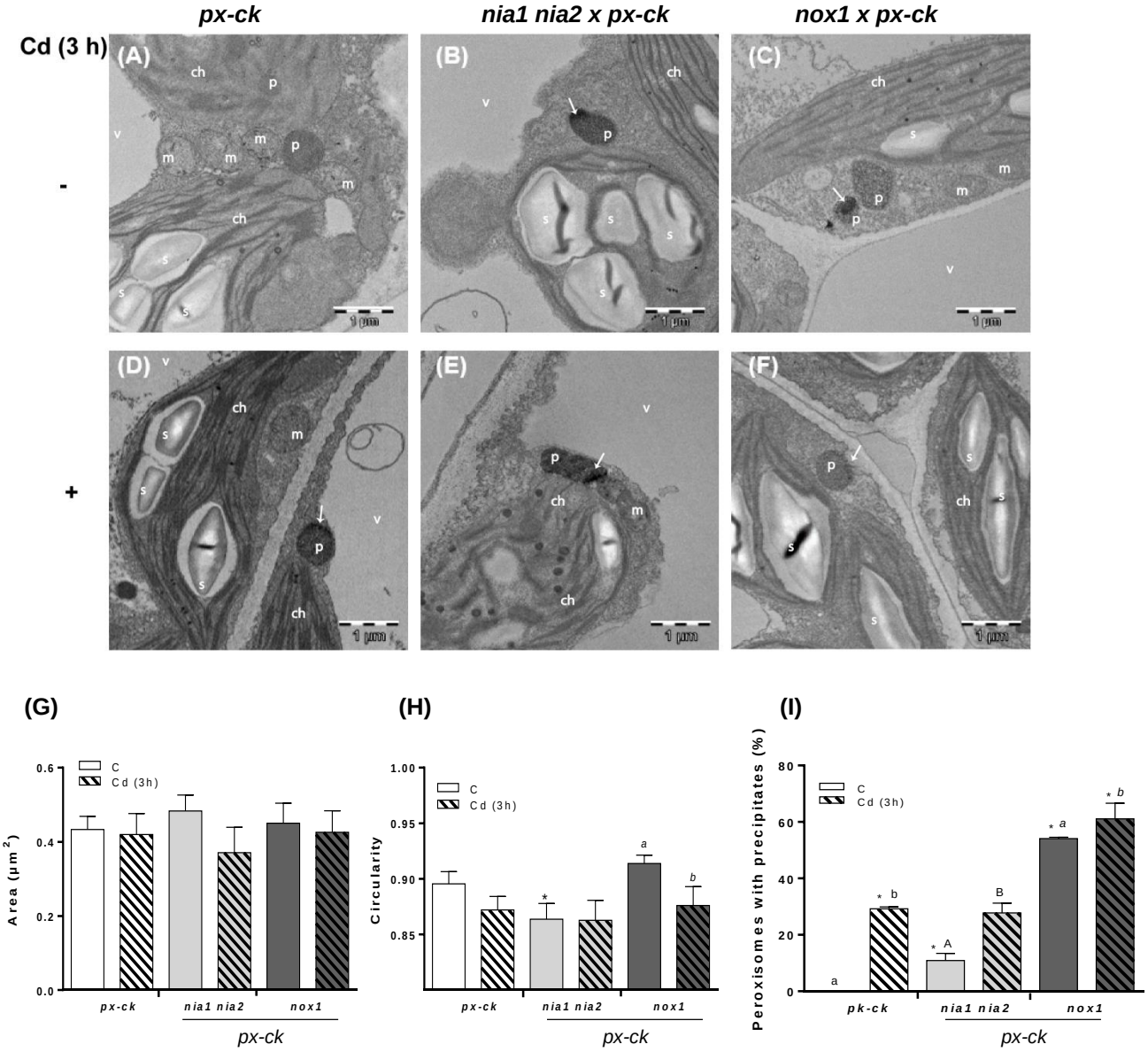
px-ck
nia1 nia2 x px-ck
nox1 x px-ck
Cd (3 h)
-
+
(A)
(B)
(C)
(D)
(E)
(F)
ch
p
v
m
s
1 µm
(G)
(H)
(I)
C
Cd (3h)
Area (µm²)
Circularity
Peroxisomes with precipitates (%)
px-ck
nia1 nia2
nox1
pk-ck

Figure 5

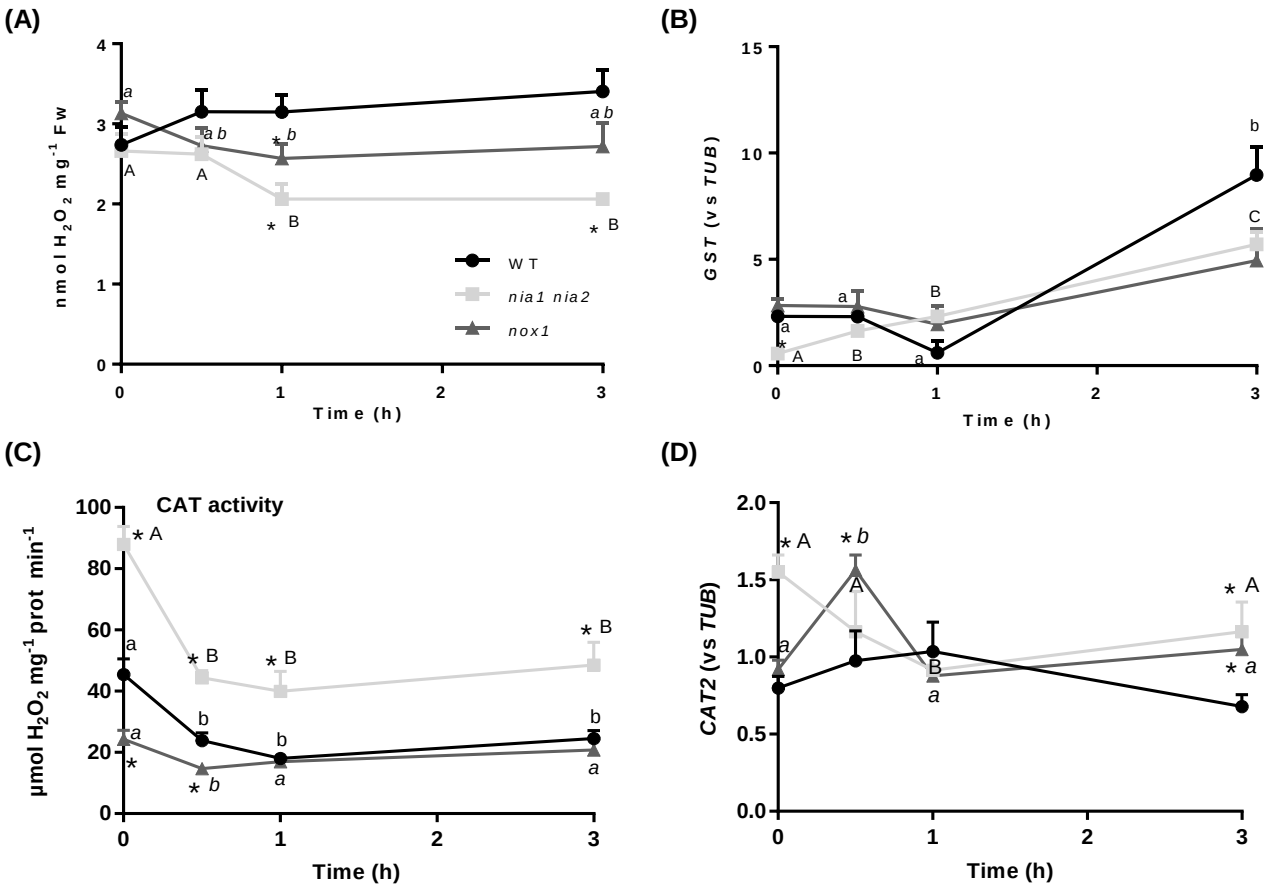
(A)
nmol H2O2 mg-1 FW
Time (h)
WT
nia1 nia2
nox1
(B)
GST (vs TUB)
Time (h)
(C)
CAT activity
µmol H2O2 mg-1 prot min-1
Time (h)
(D)
CAT2 (vs TUB)
Time (h)

Figure 6

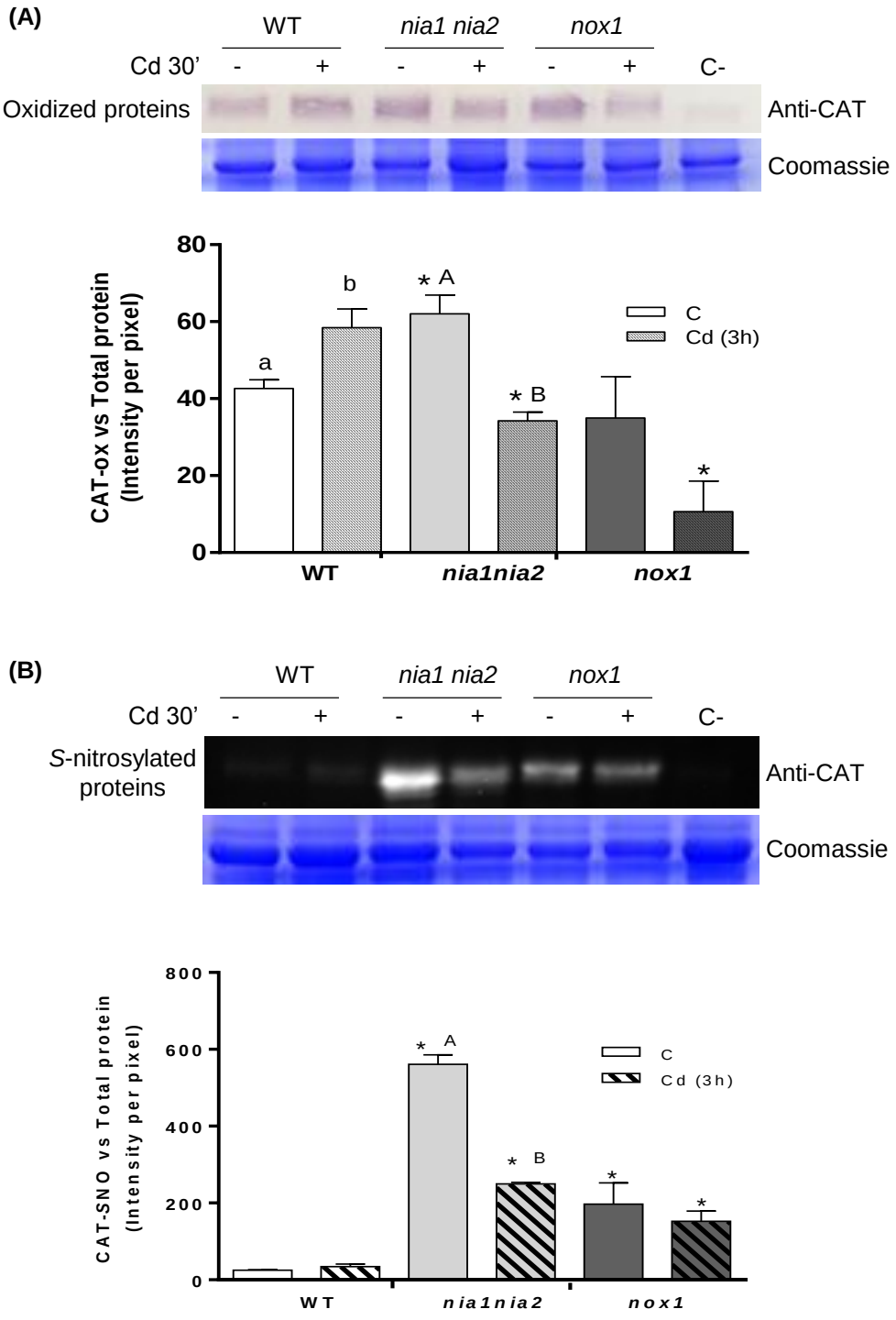
(A)
WT
nia1 nia2
nox1
Cd 30'
- + - + - + C-
Oxidized proteins
Anti-CAT
Coomassie
CAT-ox vs Total protein (Intensity per pixel)
80
60
40
20
0
a
b
* A
* B
*
C
Cd (3h)
WT
nia1nia2
nox1
(B)
WT
nia1 nia2
nox1
Cd 30'
- + - + - + C-
S-nitrosylated proteins
Anti-CAT
Coomassie
CAT-SNO vs Total protein (Intensity per pixel)
800
600
400
200
0
* A
* B
*
*
C
Cd (3h)
WT
nia1nia2
nox1

Figure 7

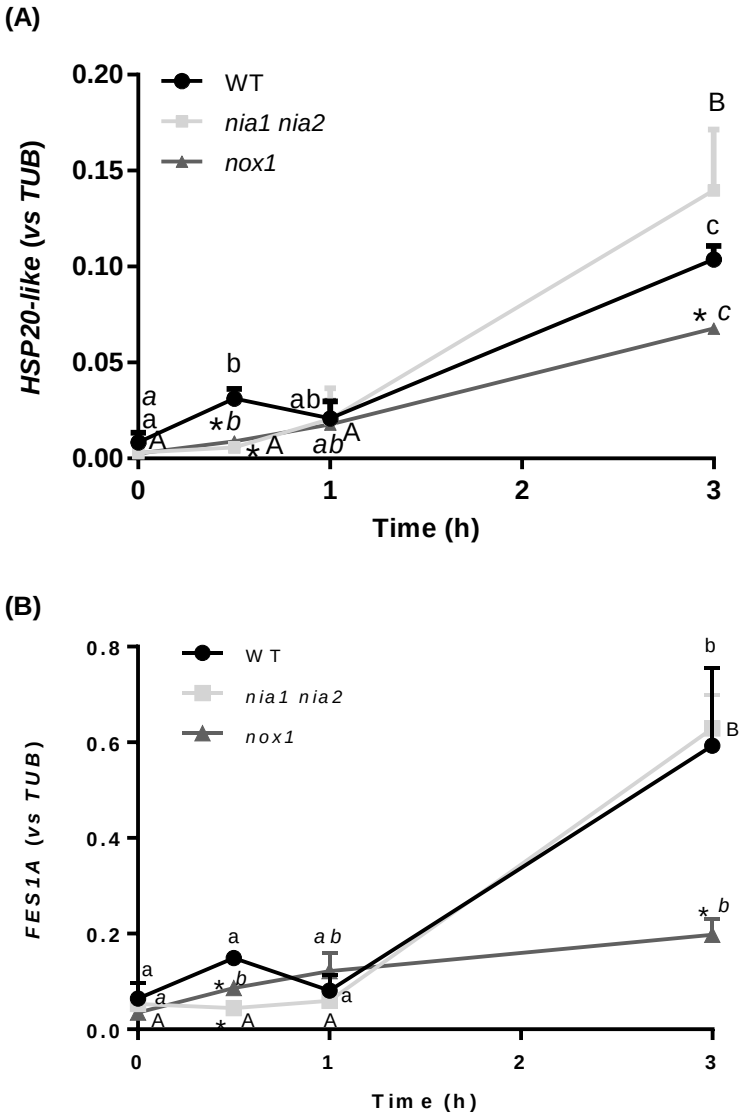
(A)
HSP20-like (vs TUB)
0.20
0.15
0.10
0.05
0.00
WT
nia1 nia2
nox1
B
c
* c
b
a
a
ab
*b
A
* A
ab A
0
1
2
3
Time (h)
(B)
FES1A (vs TUB)
0.8
0.6
0.4
0.2
0.0
W T
nia1 nia2
nox1
b
B
* b
a
a b
a
*b
a
A
* A
A
0
1
2
3
Time (h)

Figure 8

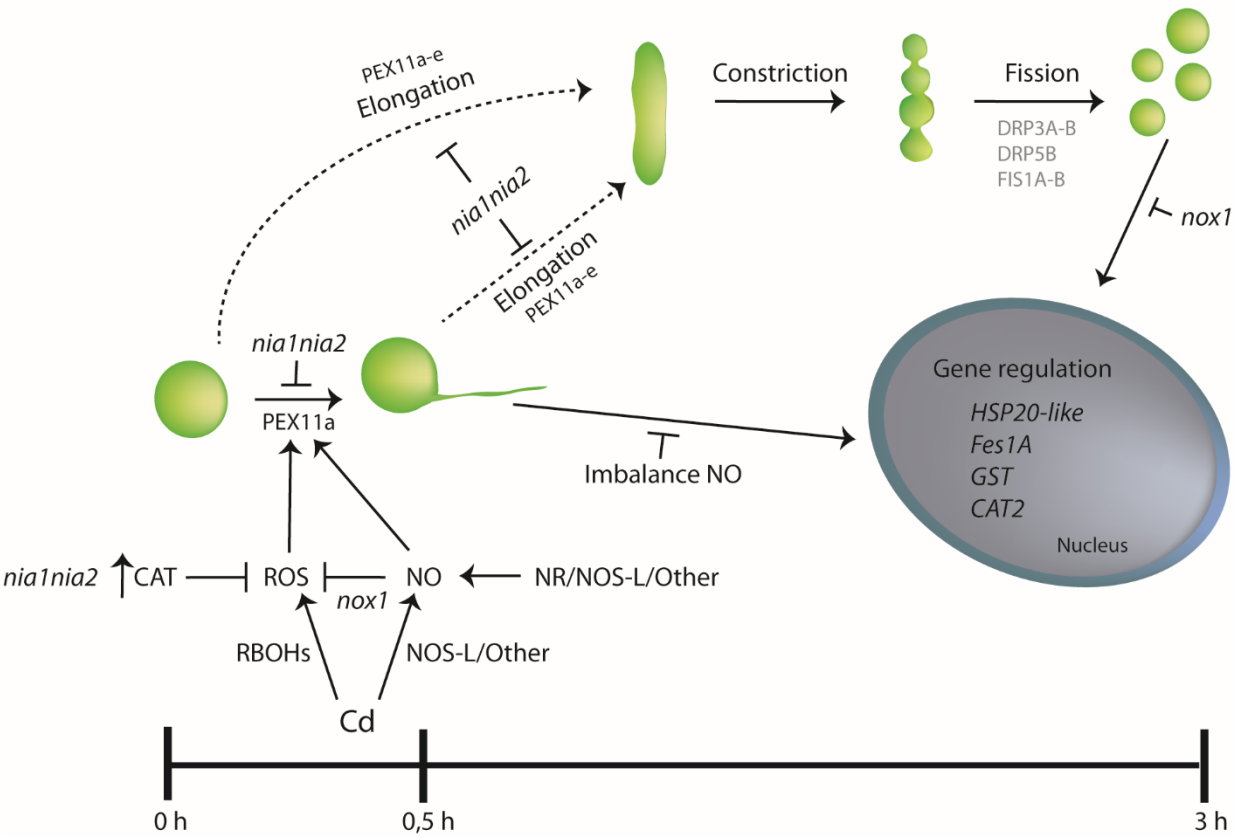
PEX11a-e
Elongation
Constriction
Fission
DRP3A-B
DRP5B
FIS1A-B
nox1
nia1nia2
Elongation
PEX11a-e
nia1nia2
PEX11a
Imbalance NO
Gene regulation
HSP20-like
Fes1A
GST
CAT2
Nucleus
nia1nia2
CAT
ROS
NO
NR/NOS-L/Other
nox1
RBOHs
NOS-L/Other
Cd
0 h
0,5 h
3 h

Figure 9